

Zeitschrift: IABSE publications = Mémoires AIPC = IVBH Abhandlungen
Band: 30 (1970)

Artikel: Grid analysis of orthotropic bridges
Autor: Heins, Conrad P. / Yoo, Chai Hong
DOI: <https://doi.org/10.5169/seals-23579>

Nutzungsbedingungen

Die ETH-Bibliothek ist die Anbieterin der digitalisierten Zeitschriften. Sie besitzt keine Urheberrechte an den Zeitschriften und ist nicht verantwortlich für deren Inhalte. Die Rechte liegen in der Regel bei den Herausgebern beziehungsweise den externen Rechteinhabern. [Siehe Rechtliche Hinweise.](#)

Conditions d'utilisation

L'ETH Library est le fournisseur des revues numérisées. Elle ne détient aucun droit d'auteur sur les revues et n'est pas responsable de leur contenu. En règle générale, les droits sont détenus par les éditeurs ou les détenteurs de droits externes. [Voir Informations légales.](#)

Terms of use

The ETH Library is the provider of the digitised journals. It does not own any copyrights to the journals and is not responsible for their content. The rights usually lie with the publishers or the external rights holders. [See Legal notice.](#)

Download PDF: 15.05.2025

ETH-Bibliothek Zürich, E-Periodica, <https://www.e-periodica.ch>

Grid Analysis of Orthotropic Bridges

Analyse des ponts orthotropes par la théorie des treillis

Trägerrostberechnung orthotroper Brücken

CONRAD P. HEINS, Jr.

Assistant Professor, Civil Engineering
Department, University of Maryland,
College Park, Md., U.S.A.

CHAI HONG YOO

Research Graduate Assistant, Civil En-
gineering Department, University of
Maryland, College Park, Md., U.S.A.

Introduction

Various analytical techniques have been proposed [1, 2, 3, 4, 5] for the analysis of orthotropic bridge structures. Most of the techniques, however, concentrate on the analysis of the stiffened deck and floor beams and neglect the interaction of the main girders. In addition to this structural assumption, the St. Venant and warping rigidities are not considered in the study of floor beams.

It is therefore proposed that a grid technique [6], utilizing an equivalent orthotropic plate analysis and finite differences [3, 7], be applied in analyzing an orthotropic bridge structure. This analysis will include both bending and torsional (St. Venant and warping) rigidities for all structural members in the system. The resulting equations are evaluated by a computer, permitting any variation in loadings and stiffnesses.

Equivalent Plate Equations

A series of interacting grids or beams, subjected to some external load q , will develop internal moments and shears. Examination of an element of the grid system, Fig. 1, describes these forces. The spacing of the grids in the x and y direction will be assumed to be $n\lambda$ and λ , respectively. All of the forces acting on the grid can now be distributed over the grid spacing, thus creating an equivalent plate system, as shown in Fig. 2.

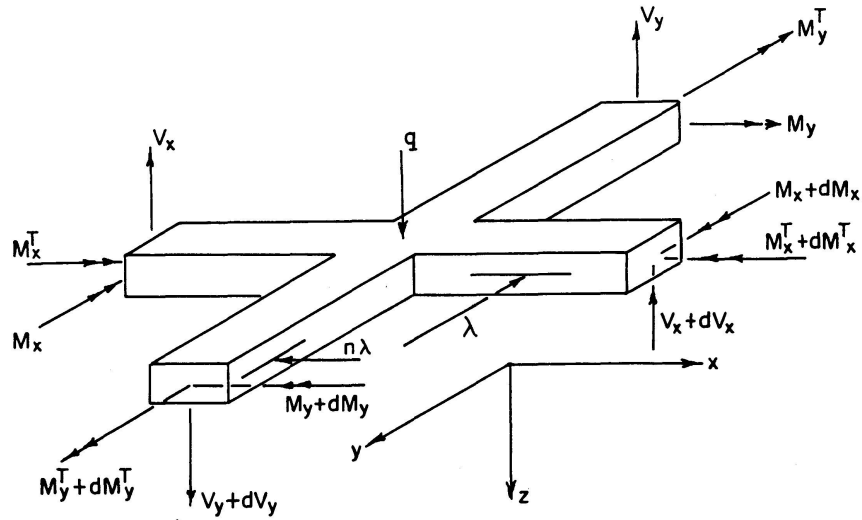


Fig. 1. Typical Grid Element.

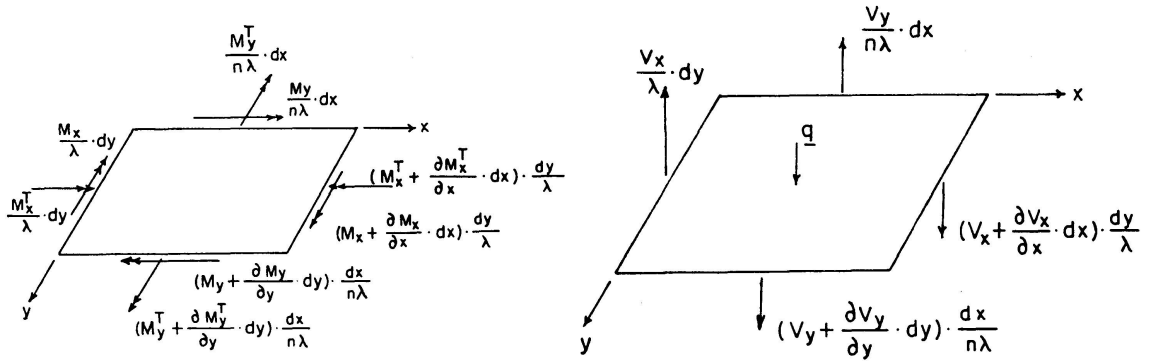


Fig. 2. Equivalent Plate Forces.

Plate Equation. – Summing forces in the z direction and moments about the x and y axis will give three equilibrium equations. These three equations can be reduced to the following general equilibrium Eq. (1).

$$\frac{1}{\lambda} \frac{\partial^2 M_x}{\partial x^2} + \left(\frac{1}{n\lambda} \frac{\partial^2 M_{Ty}}{\partial x \partial y} + \frac{1}{\lambda} \frac{\partial^2 M_{Tx}}{\partial x \partial y} \right) + \frac{1}{n\lambda} \frac{\partial^2 M_y}{\partial y^2} = -q. \quad (1)$$

The relationship between the moments (bending and torsion) and vertical deformations is now required. The bending moment and curvature equations are well known and are defined as:

$$M_x = -E I_x \frac{\partial^2 w}{\partial x^2}, \quad (2)$$

$$M_y = -E I_y \frac{\partial^2 w}{\partial y^2}. \quad (3)$$

The general torsional equation, as given in reference [7], relating total torque to rotation of a beam along the x or y axis is:

$$M_{x,y}^T = M_T^{ST} + M_T^w = G K_T \Phi' - E I_w \Phi'''. \quad (4)$$

This equation is then transformed into force by unit of width and deformation by assuming the derivatives of rotation as follows:

$$\text{Twist along } x \text{ axis:} \quad \Phi'_x = -\frac{\partial^2 w}{\partial x \partial y}. \quad (5a)$$

$$\text{Twist along } y \text{ axis:} \quad \Phi'_y = -\frac{\partial^2 w}{\partial y \partial x}. \quad (5b)$$

Taking the derivatives of Eq. (5a), (5b) and substituting these derivatives and Φ'_x and Φ'_y into (4) gives:

$$\frac{M_x^T}{\lambda} = -G \frac{K_{tx}}{\lambda} \frac{\partial^2 w}{\partial x \partial y} + E \frac{I_{wx}}{\lambda} \frac{\partial^4 w}{\partial x^3 \partial y}, \quad (6)$$

$$\frac{M_y^T}{n\lambda} = -G \frac{K_{ty}}{n\lambda} \frac{\partial^2 w}{\partial y \partial x} + E \frac{I_{wy}}{n\lambda} \frac{\partial^4 w}{\partial y^3 \partial x}. \quad (7)$$

Taking the proper derivatives of Eq. (2), (3), (6), and (7), in accordance with Eq. (1), and substituting these derivatives into Eq. (1), gives the following sixth order partial differential equation:

$$D_x \frac{\partial^4 w}{\partial x^4} - C_x \frac{\partial^6 w}{\partial x^4 \partial y^2} - C_y \frac{\partial^6 w}{\partial x^2 \partial y^4} + 2H \frac{\partial^4 w}{\partial x^2 \partial y^2} + D_y \frac{\partial^2 w}{\partial y^4} = q, \quad (8)$$

$$\text{where:} \quad D_x = \frac{E I_x}{\lambda}, \quad C_x = \frac{E I_{wx}}{\lambda}, \quad 2H = G \left(\frac{K_{tx}}{\lambda} + \frac{K_{ty}}{n\lambda} \right), \quad (9)$$

$$D_y = \frac{E I_y}{n\lambda}, \quad C_y = \frac{E I_{wy}}{n\lambda}.$$

Force Equations. — Utilizing the previous equations, the general force equations on each beam corresponding to Fig. 1, can now be evaluated.

Bending Moment Equations:

$$M_x = -D_x \frac{\partial^2 w}{\partial x^2}, \quad (10a)$$

$$M_y = -D_y \frac{\partial^2 w}{\partial y^2}. \quad (10b)$$

Shear Equations:

$$V_x = -D_x \frac{\partial^3 w}{\partial x^3} - H_y \frac{\partial^3 w}{\partial x \partial y^2} + C_y \frac{\partial^5 w}{\partial x \partial y^4}, \quad (11a)$$

$$V_y = -D_y \frac{\partial^3 w}{\partial y^3} - H_x \frac{\partial^3 w}{\partial y \partial x^2} + C_x \frac{\partial^5 w}{\partial y \partial x^4}. \quad (11b)$$

Reaction Equations:

$$R_x = -D_x \left[\frac{\partial^3 w}{\partial x^3} + \frac{2H}{D_x} \frac{\partial^3 w}{\partial x \partial y^2} - \frac{C_x}{D_x} \frac{\partial^5 w}{\partial x^3 \partial y^2} - \frac{C_y}{D_x} \frac{\partial^5 w}{\partial x \partial y^4} \right], \quad (12a)$$

$$R_y = -D_y \left[\frac{\partial^3 w}{\partial y^3} + \frac{2H}{D_y} \frac{\partial^3 w}{\partial y \partial x^2} - \frac{C_y}{D_y} \frac{\partial^5 w}{\partial y^3 \partial x^2} - \frac{C_x}{D_y} \frac{\partial^5 w}{\partial y \partial x^4} \right]. \quad (12b)$$

Torsional Moment Equations:

$$M_x^T = -H_x \left[\frac{\partial^2 w}{\partial x \partial y} - \frac{C_x}{H_x} \frac{\partial^4 w}{\partial x^3 \partial y} \right], \quad (13a)$$

$$M_y^T = -H_y \left[\frac{\partial^2 w}{\partial x \partial y} - \frac{C_y}{H_y} \frac{\partial^4 w}{\partial y^3 \partial x} \right], \quad (13b)$$

$$M_{Tx}^{ST} = -H_x \left[\frac{\partial^2 w}{\partial x \partial y} \right], \quad (14a)$$

$$M_{Tx}^v = C_x \left[\frac{\partial^4 w}{\partial x^3 \partial y} \right], \quad (14b)$$

$$M_{Ty}^{ST} = -H_y \left[\frac{\partial^2 w}{\partial x \partial y} \right], \quad (15a)$$

$$M_{Ty}^v = C_y \left[\frac{\partial^4 w}{\partial y^3 \partial x} \right]. \quad (15b)$$

Rotation Function Φ'' :

$$\Phi_x'' = -\frac{\partial^3 w}{\partial x^2 \partial y}, \quad (16a)$$

$$\Phi_y'' = -\frac{\partial^3 w}{\partial y^2 \partial x}. \quad (16b)$$

where the constants associated with Eqs.(10) through (16) are defined by Eq. (9) and the following Eq. (17):

$$H_x = G \frac{K_{tx}}{\lambda}, \quad H_y = G \frac{K_{ty}}{n\lambda}. \quad (17)$$

Solution of Orthotropic Plate Equation

The solution of the differential equation (8) is obtained by use of the finite difference technique. This technique requires the selection of discrete points throughout the equivalent plate element.

Examining Fig. 3, a set of coordinates and points are described on a plate, with mesh spacings of $n\lambda$ and λ along the x and y axes respectively. These spacings also correspond to the grid spacing described in Fig.1. Using the difference relationships for the partial derivatives, the finite difference solution of the differential equation (8) is obtained and results in Eq.(18).

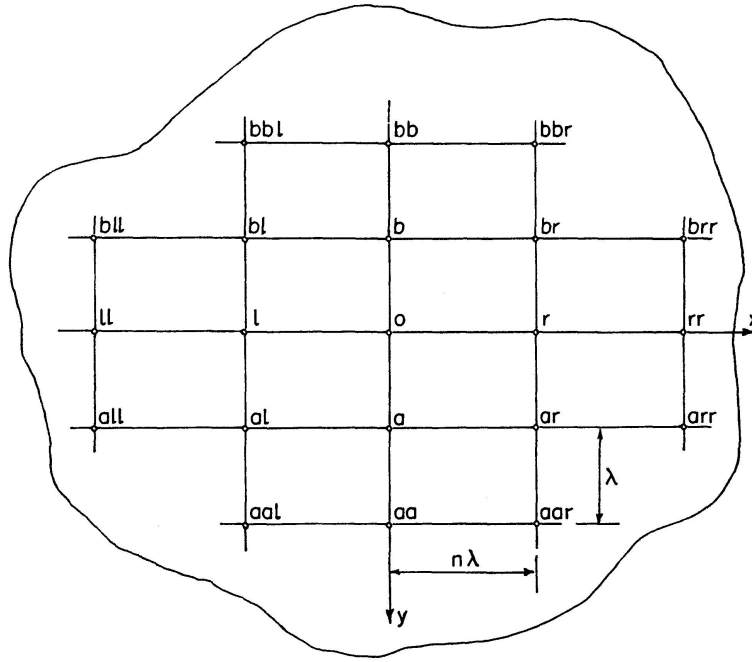


Fig. 3. Typical Mesh Pattern Array.

$$\begin{aligned}
& w_o [6n^4 + 6(\beta/\alpha)^2 + 8n^2\beta + 12A + 12n^2B] \\
& - 4(w_r + w_l) [n^2\beta + (\beta/\alpha)^2 + 2A + 6/4n^2B] \\
& - 4(w_a + w_b) [n^2\beta + n^4 + 6/4A + 2n^2B] \\
& + (w_{rr} + w_{ll}) [(\beta/\alpha)^2 + 2A] + (w_{aa} + w_{bb}) [n^4 + 2n^2B] \\
& + (w_{ar} + w_{br} + w_{al} + w_{bl}) [2n^2\beta + 4A + 4n^2B] \\
& - A(w_{all} + w_{bll} + w_{arr} + w_{brr}) - n^2B(w_{aar} + w_{aal} - w_{bbr} + w_{bbl}) = \frac{qn^4\lambda^4}{D_y},
\end{aligned} \tag{18}$$

$$\text{where } \alpha = H/\sqrt{D_x D_y}, \quad \beta = H/D_y, \quad A = C_x/\lambda^2 D_y, \quad B = C_y/\lambda^2 D_y. \tag{19}$$

The force equations, (10) through (15), and rotation functions Eq. (16), can also be evaluated in finite difference form. Defining the following constants:

$$\begin{aligned}
\Phi_{yx} &= \frac{H_y}{D_x}, & \eta_y &= \frac{C_y}{\lambda^2 D_x}, & \xi_y &= \frac{H}{D_y}, & \epsilon_y &= \frac{C_y}{\lambda^2 H_y}, \\
\Phi_{xy} &= \frac{H_x}{D_y}, & \eta_x &= \frac{C_x}{\lambda^2 D_y}, & \xi_x &= \frac{H}{D_x}, & \epsilon_x &= \frac{C_x}{\lambda^2 H_x}.
\end{aligned} \tag{20}$$

Equations (1) through (16) are described in a finite difference mesh pattern as shown in Figs. 5 through 18.

These relationships are now used to modify the general Eq. (18), in order to accommodate the various boundary conditions for a bridge structure. The modifications and the resulting load-deformation mesh patterns will now be described.

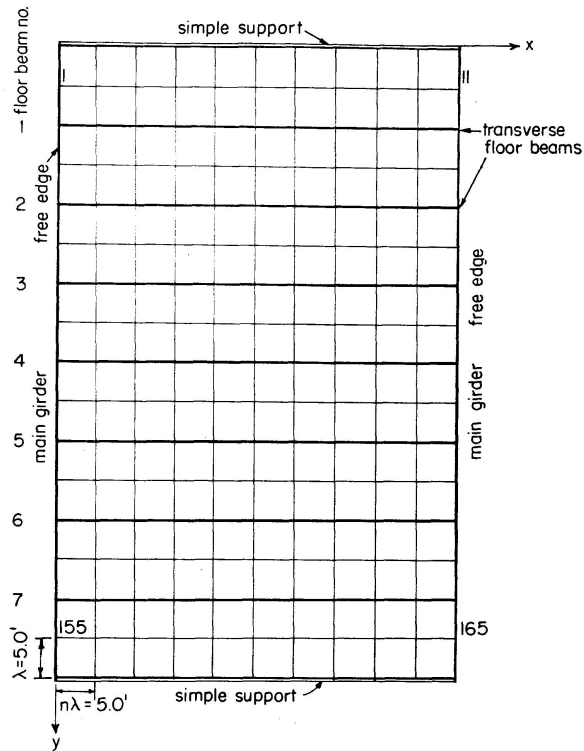


Fig. 4. Bridge Mesh Pattern.

$$\left(-\frac{D_x}{n^2 \lambda^2} \right) \cdot w \cdot \left[\begin{array}{c} \boxed{1} \\ \boxed{-2} \\ \boxed{1} \end{array} \right] = M_x$$

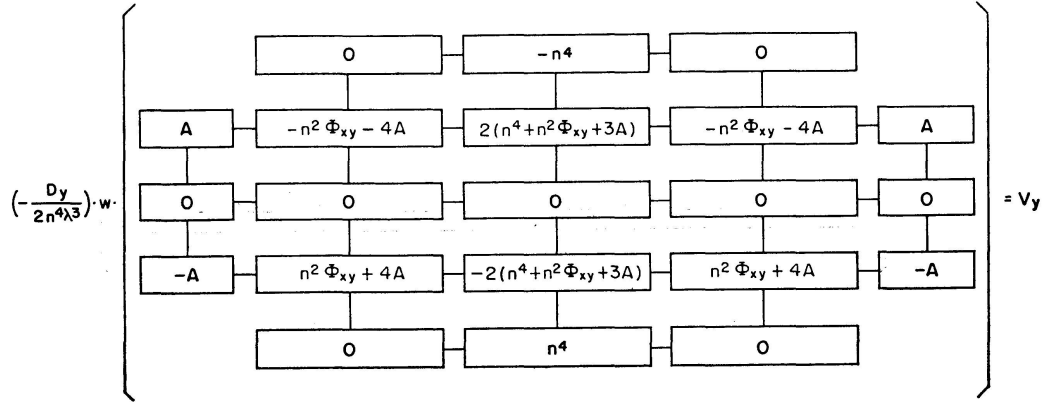
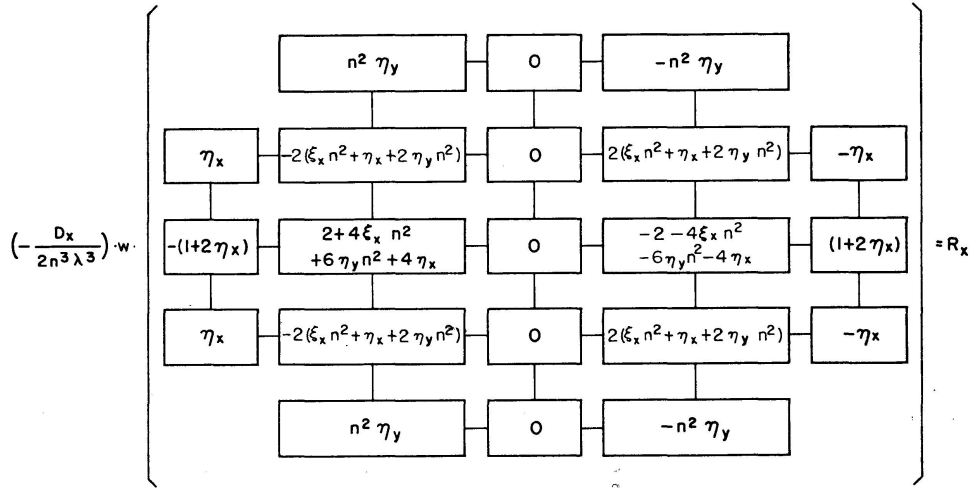
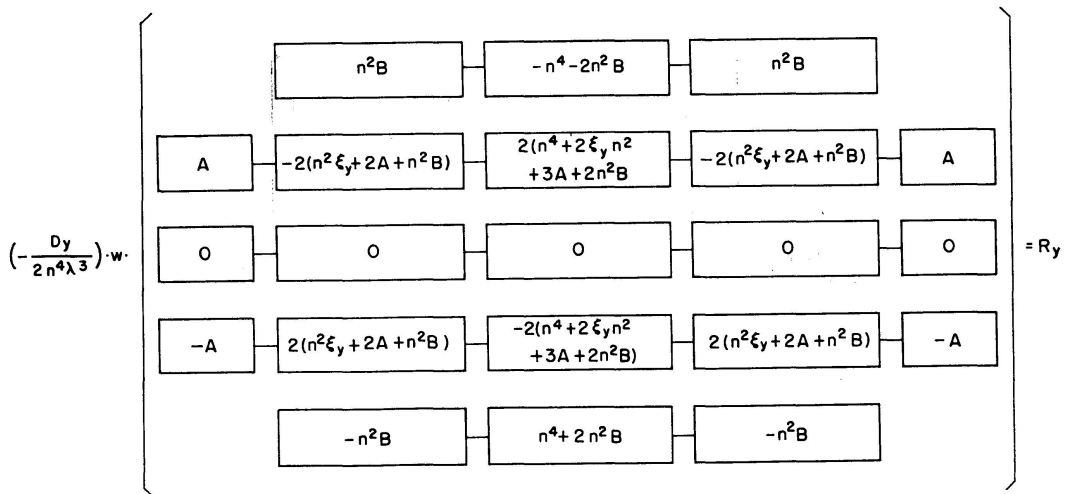
Fig. 5. M_x General Mesh Pattern.

$$\left(-\frac{D_y}{\lambda^2} \right) \cdot w \cdot \left[\begin{array}{c} \boxed{1} \\ \boxed{-2} \\ \boxed{1} \end{array} \right] = M_y$$

Fig. 6. M_y General Mesh Pattern.

$$\left(-\frac{D_x}{2n^3 \lambda^3} \right) \cdot w \cdot \left[\begin{array}{ccccc} \boxed{n^2 \eta_y} & \boxed{0} & \boxed{-n^2 \eta_y} & & \\ \boxed{0} & \boxed{-n^2(\Phi_{yx} + 4\eta_y)} & \boxed{0} & \boxed{n^2(\Phi_{yx} + 4\eta_y)} & \boxed{0} \\ \boxed{-1} & \boxed{2 + 2n^2(\Phi_{yx} + 3\eta_y)} & \boxed{0} & \boxed{-2 - 2n^2(\Phi_{yx} + 3\eta_y)} & \boxed{1} \\ \boxed{0} & \boxed{-n^2(\Phi_{yx} + 4\eta_y)} & \boxed{0} & \boxed{n^2(\Phi_{yx} + 4\eta_y)} & \boxed{0} \\ \boxed{n^2 \eta_y} & \boxed{0} & \boxed{-n^2 \eta_y} & & \end{array} \right] = V_x$$

Fig. 7. V_x General Mesh Pattern.

Fig. 8. V_y General Mesh Pattern.Fig. 9. R_x General Mesh Pattern.Fig. 10. R_y General Mesh Pattern.

$$\left(-\frac{H_x}{4n^3\lambda^2} \right) \cdot w \cdot \begin{pmatrix} \boxed{-\epsilon_x} & \boxed{n^2+2\epsilon_x} & \boxed{0} & \boxed{-n^2-2\epsilon_x} & \boxed{\epsilon_x} \\ \boxed{0} & \boxed{0} & \boxed{0} & \boxed{0} & \boxed{0} \\ \boxed{\epsilon_x} & \boxed{-n^2-2\epsilon_x} & \boxed{0} & \boxed{n^2+2\epsilon_x} & \boxed{-\epsilon_x} \end{pmatrix} = M_x^T$$

Fig. 11. M_x^T General Mesh Pattern.

$$\left(-\frac{H_x}{4n\lambda^2} \right) \cdot w \cdot \begin{pmatrix} \boxed{1} & \boxed{0} & \boxed{-1} \\ \boxed{0} & \boxed{0} & \boxed{0} \\ \boxed{-1} & \boxed{0} & \boxed{1} \end{pmatrix} = M_{Tx}^{ST}$$

Fig. 12. M_{Tx}^{ST} General Mesh Pattern.

$$\left(-\frac{C_x}{4n^3\lambda^4} \right) \cdot w \cdot \begin{pmatrix} \boxed{-1} & \boxed{2} & \boxed{0} & \boxed{-2} & \boxed{1} \\ \boxed{0} & \boxed{0} & \boxed{0} & \boxed{0} & \boxed{0} \\ \boxed{1} & \boxed{-2} & \boxed{0} & \boxed{2} & \boxed{-1} \end{pmatrix} = M_{Tx}^w$$

Fig. 13. M_{Tx}^w General Mesh Pattern.

$$\left(-\frac{H_y}{4n\lambda^2} \right) \cdot w \cdot \begin{pmatrix} \boxed{-\epsilon_y} & \boxed{0} & \boxed{\epsilon_y} \\ \boxed{1+2\epsilon_y} & \boxed{0} & \boxed{-1-2\epsilon_y} \\ \boxed{0} & \boxed{0} & \boxed{0} \\ \boxed{-1-2\epsilon_y} & \boxed{0} & \boxed{1+2\epsilon_y} \\ \boxed{\epsilon_y} & \boxed{0} & \boxed{-\epsilon_y} \end{pmatrix} = M_y^T$$

Fig. 14. M_y^T General Mesh Pattern.

$$\left(-\frac{H_y}{4n\lambda^2} \right) \cdot w \cdot \begin{pmatrix} \boxed{1} & \boxed{0} & \boxed{-1} \\ \boxed{0} & \boxed{0} & \boxed{0} \\ \boxed{-1} & \boxed{0} & \boxed{1} \end{pmatrix} = M_{Ty}^{ST}$$

 Fig. 15. M_{Ty}^{ST} General Mesh Pattern.

$$\left(-\frac{C_y}{4n\lambda^4} \right) \cdot w \cdot \begin{pmatrix} \boxed{-1} & \boxed{0} & \boxed{1} \\ \boxed{2} & \boxed{0} & \boxed{-2} \\ \boxed{0} & \boxed{0} & \boxed{0} \\ \boxed{-2} & \boxed{0} & \boxed{2} \\ \boxed{1} & \boxed{0} & \boxed{-1} \end{pmatrix} = M_{Ty}^w$$

 Fig. 16. M_{Ty}^w General Mesh Pattern.

$$\left(-\frac{1}{2n^2\lambda^3} \right) \cdot w \cdot \begin{pmatrix} \boxed{-1} & \boxed{2} & \boxed{-1} \\ \boxed{0} & \boxed{0} & \boxed{0} \\ \boxed{1} & \boxed{-2} & \boxed{1} \end{pmatrix} = \Phi_x''$$

 Fig. 17. Φ_x'' General Mesh Pattern.

$$\left(-\frac{1}{2n\lambda^3} \right) \cdot w \cdot \begin{pmatrix} \boxed{-1} & \boxed{0} & \boxed{1} \\ \boxed{2} & \boxed{0} & \boxed{-2} \\ \boxed{-1} & \boxed{0} & \boxed{1} \end{pmatrix} = \Phi_y''$$

 Fig. 18. Φ_y'' General Mesh Pattern.

Mesh Patterns

The general structural problem which will be evaluated consists of a series of interconnected deck, floor beam, and main girder comprising a bridge system. This bridge is simply supported at two ends and has two free supports, as described in Fig. 4.

Six general finite difference mesh patterns are therefore required to accommodate this model.

Mesh Condition 1. General Interior Load Point

The general mesh pattern for any load point completely within the boundaries is described in Fig. 19, and is Eq. (18), written in mesh pattern form.

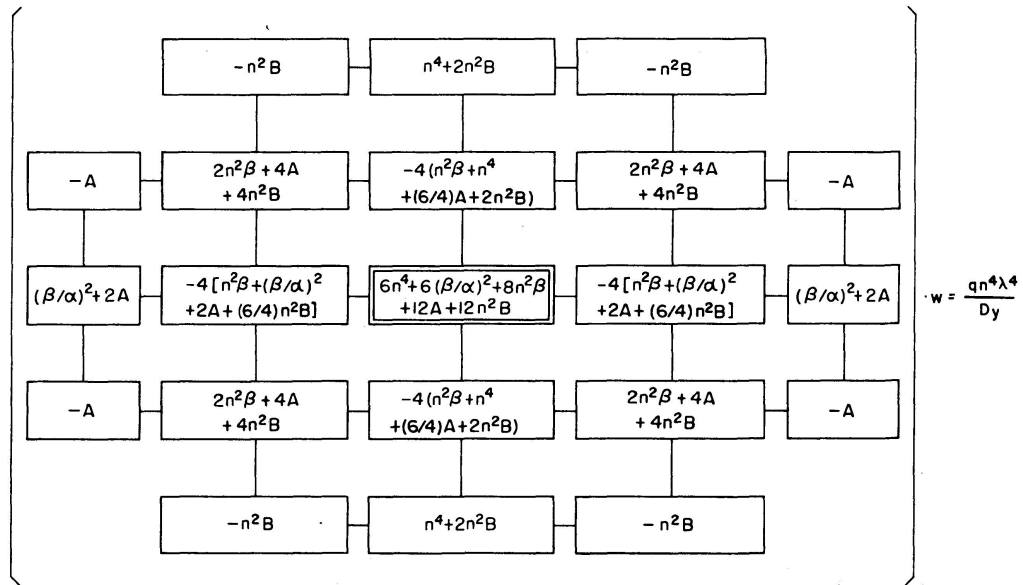


Fig. 19. Mesh Condition No. 1.

Mesh Condition 2. Load Point Adjacent to Simple Support

This type of loading requires three boundary conditions in order to express the three mesh points beyond the boundary relative to known mesh points. This relationship can be obtained by the expression $M_y = 0$. Applying this equation along the simple supports, at three locations, and substituting these relationships into Eq. (18) or Fig. 19 gives mesh condition 2, Fig. 20.

Mesh Condition 3. Load Point Adjacent to Free Support

This condition also requires three boundary conditions, in order to relate interior and exterior points. The relationship for all three boundary conditions is $M_x = 0$ at each required point along the free edge. Applying this equation

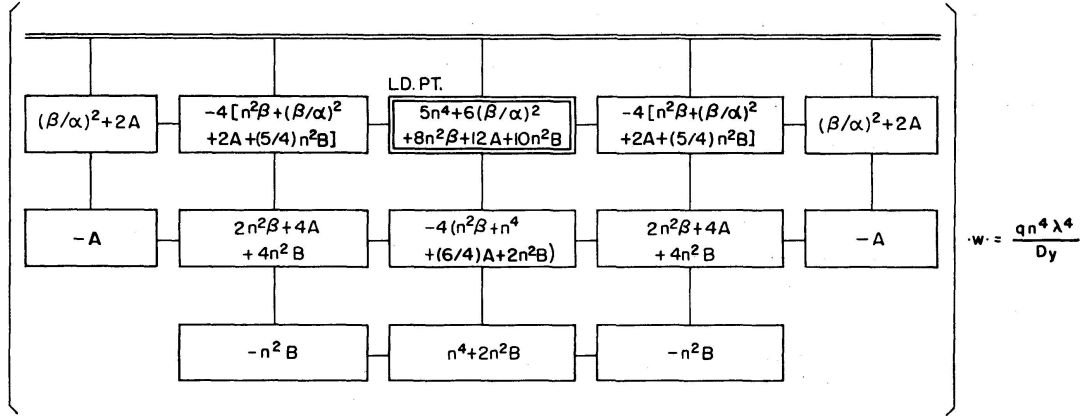


Fig. 20. Mesh Condition No. 2.

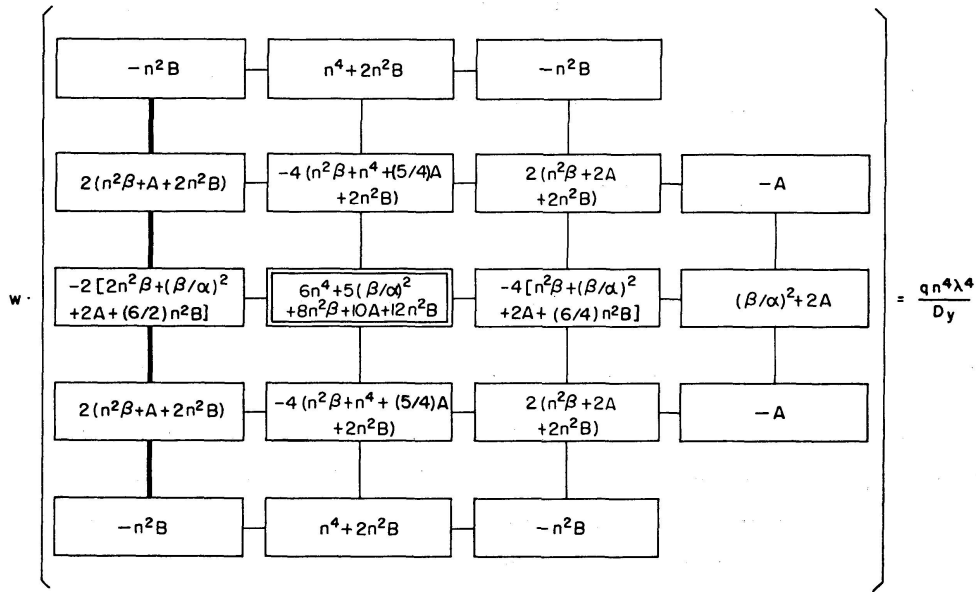


Fig. 21. Mesh Condition No. 3.

and substituting the results into Eq. (18) gives the final mesh condition 3, Fig. 21.

Mesh Condition 4. Load Point on a Free Support

This loading condition requires eight boundary conditions. The boundary conditions that were used are:

1. $M_x = 0$ for five mesh points.
2. $R_x = 0$ for one mesh point.
3. $\left(\frac{\partial w}{\partial x}\right)_l = \frac{1}{2} \left[\left(\frac{\partial w}{\partial x}\right)_{al} + \left(\frac{\partial w}{\partial x}\right)_{bl} \right]$ one mesh point.
4. $\left(\frac{\partial w}{\partial y}\right)_l = \frac{1}{2} \left[\left(\frac{\partial w}{\partial y}\right)_o + \left(\frac{\partial w}{\partial y}\right)_u \right]$ one mesh point.

The first two types of boundary conditions, for a free edge, are self-explanatory. The last two conditions are relationships relating the slope at a given

point to the sum of the average slopes surrounding that point. These slope equations were required in order to express *all* exterior points relative to the interior points. The results from all of the eight boundary conditions, and their substitution, gives mesh condition 4, Fig. 22.

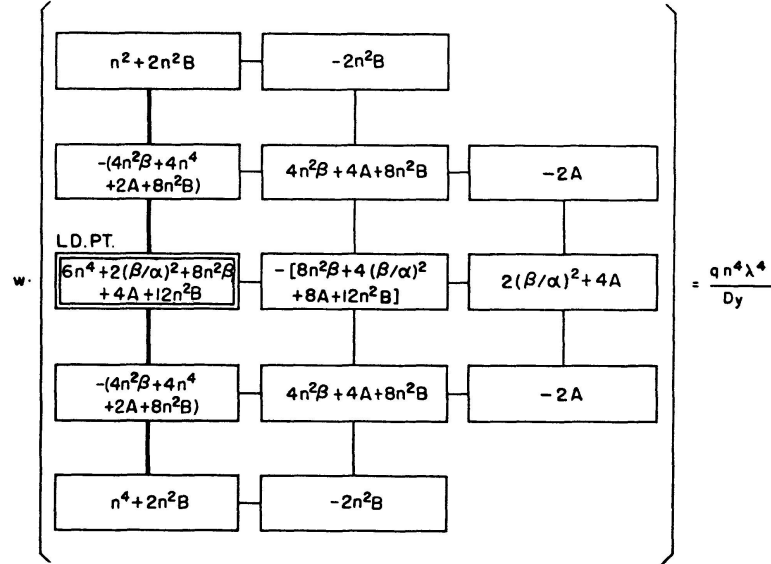


Fig. 22. Mesh Condition No. 4.

Mesh Condition 5. Load Point Adjacent to a Simple and Free Support

This load condition requires six boundary conditions. As utilized in mesh conditions 2 and 3, the moments $M_y = 0$ along the simple support and $M_x = 0$ along the free support are used. The solution of these conditions, when substituted into Eq. (18), results in mesh Fig. 23.

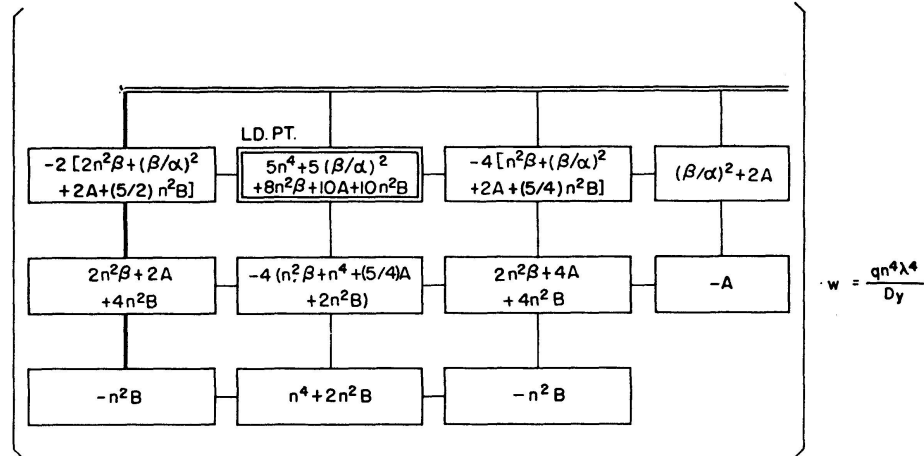


Fig. 23. Mesh Condition No. 5.

Mesh Condition 6. Load Point Adjacent to a Simple Support on a Free Support

There are ten boundary conditions that are required for this loading condition. The required relationships are:

1. $M_y = 0$ at two points.
2. $M_x = 0$ at four points.
3. $\left(\frac{\partial w}{\partial y}\right)_a = \frac{1}{2} \left[\left(\frac{\partial w}{\partial y}\right)_{ar} + \left(\frac{\partial w}{\partial y}\right)_{al} \right]$.
4. $\left(\frac{\partial w}{\partial y}\right)_l = \frac{1}{2} \left[\left(\frac{\partial w}{\partial y}\right)_o + \left(\frac{\partial w}{\partial y}\right)_n \right]$.
5. $\left(\frac{\partial w}{\partial x}\right)_l = \frac{1}{2} \left[\left(\frac{\partial w}{\partial x}\right)_{al} + \left(\frac{\partial w}{\partial x}\right)_{bl} \right]$.
6. $R_x = 0$ at one point.

The solution of these ten equations, and their relationships, results in mesh condition 6, Fig. 24.

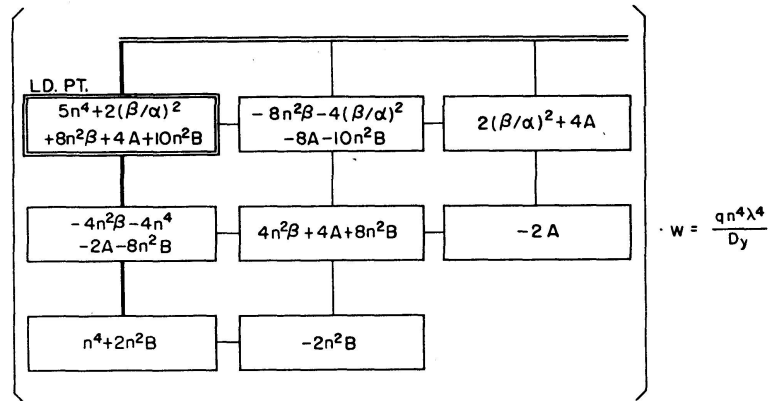


Fig. 24. Mesh Condition No. 6.

With all of the required mesh patterns defined and developed, the solution of any given loaded bridge grid system can be solved. The generation of the required equations and their solutions has been accomplished by a computer program (8). The evaluation of deflection at each grid point will then permit evaluation of each force at that grid point. The force equations (10) through (16), as described in Figs. 5 through 18, have also been modified to account for the boundary conditions, and these various equations are then evaluated by a computer program. The two basic computer programs that have been written will evaluate deflections and then forces.

Stresses

For any given bridge system and loading, the deflections are obtained by solving the set of simultaneous difference equations, as represented by mesh conditions 1 through 6. The solutions of these equations yields deformations at each respective girder mesh point. These deformations are then utilized to evaluate forces, given by Eqs. (10) through (16). With these forces, the stresses throughout the system can be determined by the following equations:

Bending: $\sigma_{bx,y} = \frac{M_{x,y}}{S},$ (21)

where: M_x Eq. (10a), Fig. 5, M_y Eq. (10b), Fig. 6.

Normal Warping: $\sigma_{wx,y} = E W_{nsx} \Phi_x''$ or $E W_{nsy} \Phi_y'',$ (22)

where: Φ_x'' Eq. (16a), Fig. 17, Φ_y'' Eq. (16b), Fig. 18.

St. Venant Shear: $\tau_{STx,y} = M_{Tx}^{ST} \frac{t}{K_{tx}}$ or $M_{Ty}^{ST} \frac{t}{K_{ty}},$ (23)

where: M_{Tx}^{ST} Eq. (14a), Fig. 12, M_{Ty}^{ST} Eq. (15a), Fig. 15.

Warping Shear: $\tau_{wx,y} = M_{Tx}^w \frac{S_{wsx}}{t I_{wx}}$ or $M_{Ty}^w \frac{S_{wsy}}{t I_{wy}},$ (24)

where: M_{Tx}^w Eq. (14b), Fig. 13, M_{Ty}^w Eq. (15b), Fig. 16.

Bending Shear: $\tau_{bx,y} = V_x \frac{Q_x}{I_x t}$ or $V_y \frac{Q_y}{I_y t},$ (25)

where: V_x Eq. (11a), Fig. 7, V_y Eq. (11b), Fig. 8.

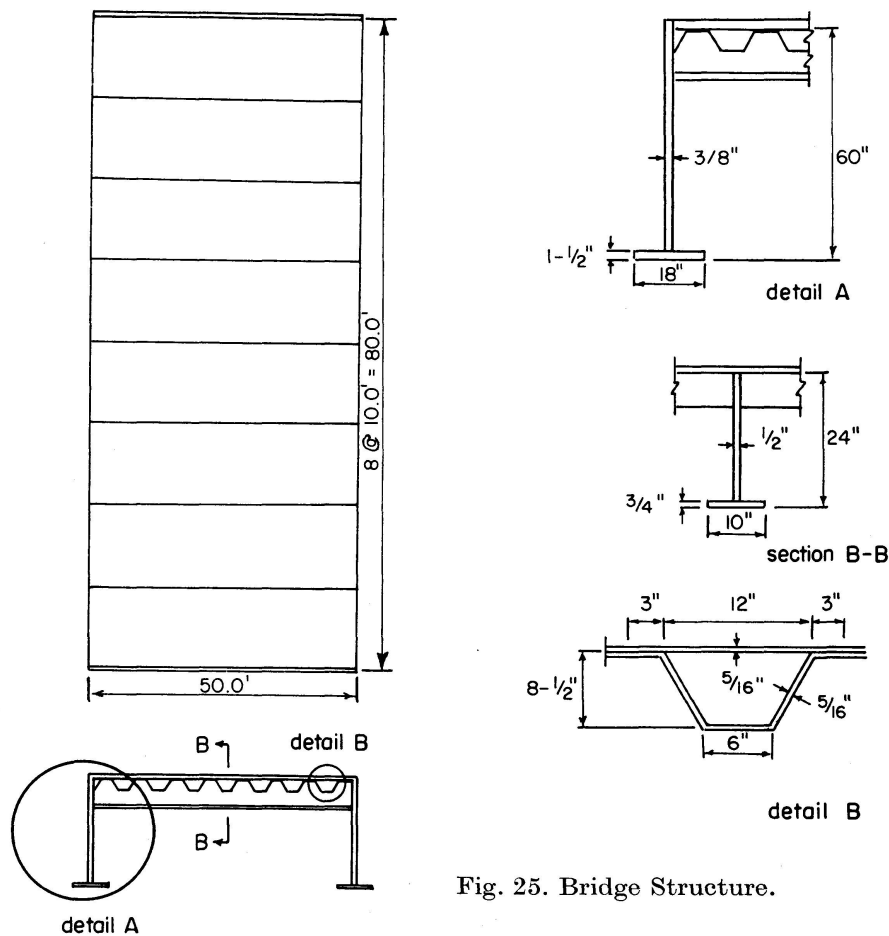


Fig. 25. Bridge Structure.

Bridge Solution

The following will describe the analysis of a hypothetical orthotropic bridge, subjected to a given truck loading. This structure, Fig. 25, consists of a cellular deck framing into transverse floor beams and two outside main longitudinal girders. The stiffnesses of the various elements of the bridge systems were evaluated at the respective intersections of the grid nodes, described in

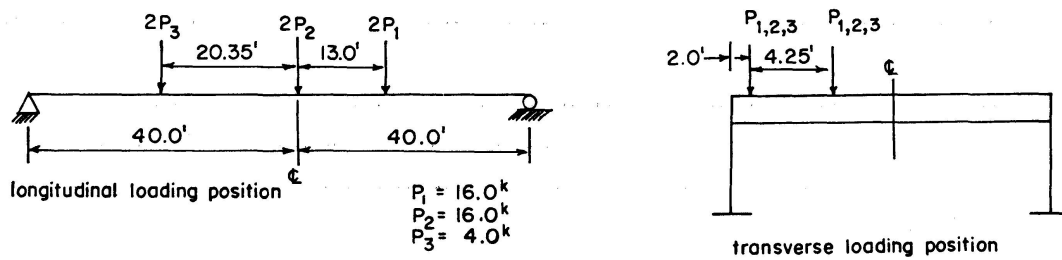


Fig. 26. Loading Condition.

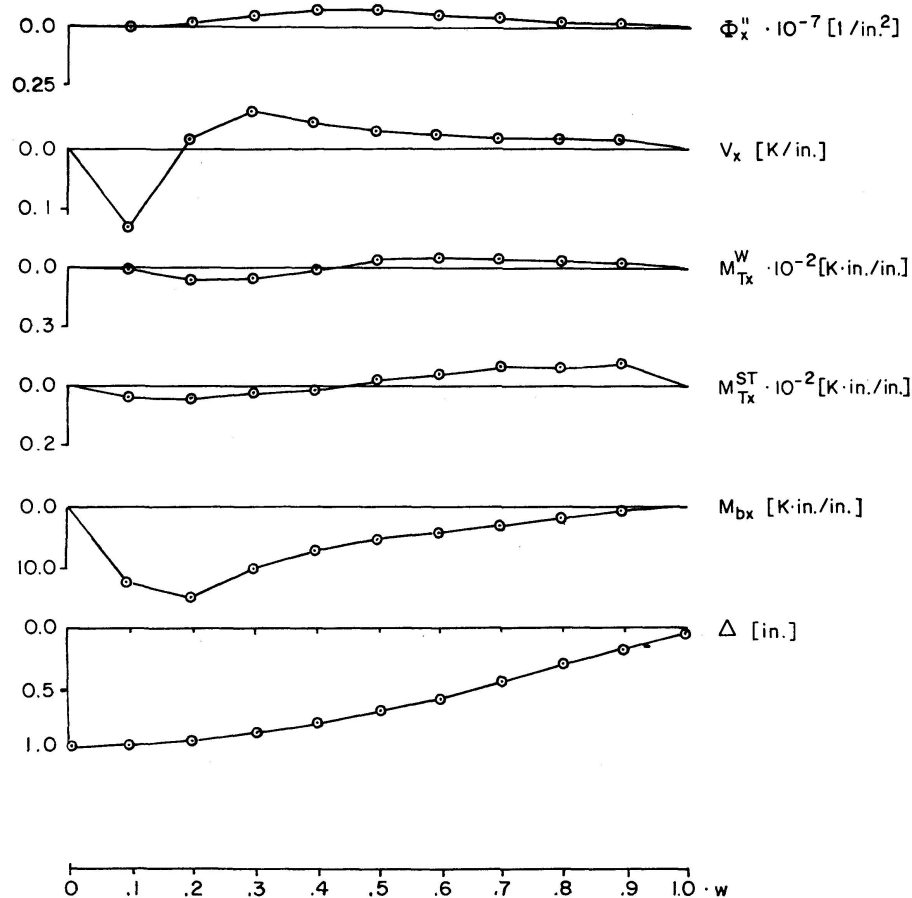


Fig. 27. Forces and Distortions along Floor Beam No. 4.

Fig. 4. A total of 165 grid points were selected for this analysis. The stiffnesses, D_x , D_y , H_x , H_y , C_x and C_y were then computed for the

- a) Longitudinal Deck
- b) Transverse Deck
- c) Transverse Floor Beam
- d) Longitudinal Main Girder

at the respective points, as listed in Ref. [8].

With these stiffnesses and specified loading, Fig. 26, the bridge deflections at each grid point were determined. These deflections were then used to evaluate forces in the system.

Fig. 27 describes the resulting deflection Δ , shear V_x , bending moment M_{bx} , torsional moments M_{Tx}^{ST} , M_{Tx} and torsional function Φ_x'' along floor beam number 4. Similar results were obtained for the remaining girders 1 through 7, for this loading case.

Fig. 28 describes similar results for the left main longitudinal girder.

These data are typical of the values obtained for the many loading cases which were investigated (8). From these data the resulting stresses, as prescribed by equations (21) through (25) throughout the system, can then be evaluated.

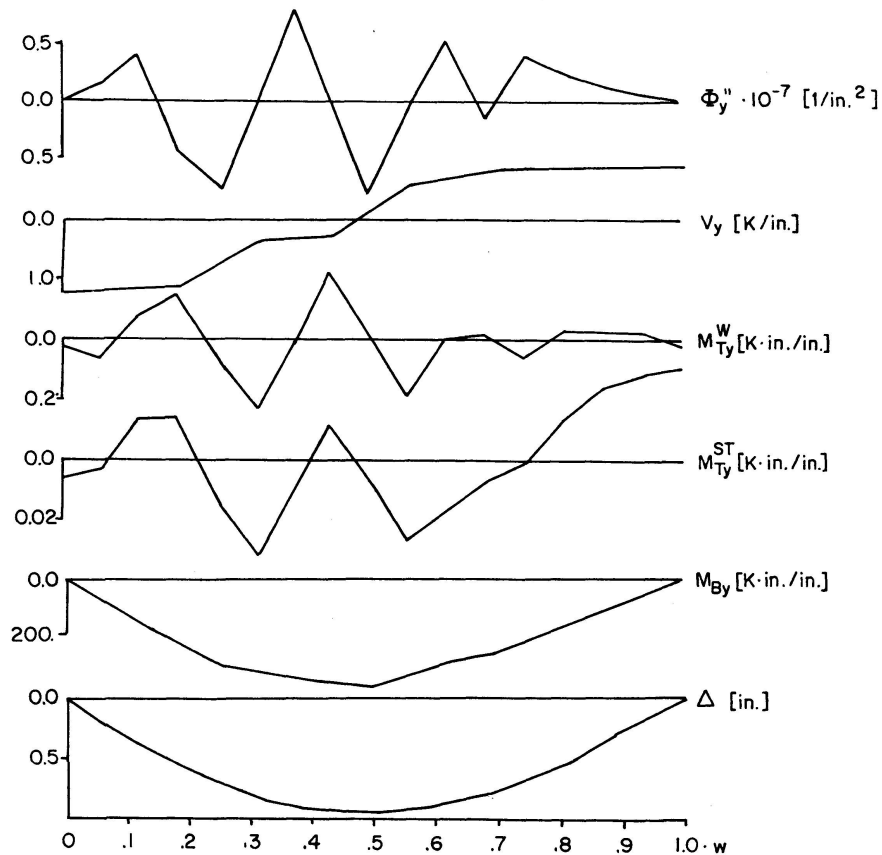


Fig. 28. Forces and Distortions along Left Main Girder.

Nomenclature

q	Mesh point load intensity – force per unit area
x, y	Horizontal rectangular coordinates. The origin of coordinates is always at the left corner of the simply supported edge of the plate. The x -axis is always parallel to the pair of simply supported edges of the plate
z	Vertical coordinate, positive downward
w	Deflection of the plate, positive downward
$\lambda y = \lambda$	Spacing of a grid in the y direction – in.
$\lambda x = n \lambda$	Spacing of a grid in the x direction – in.
$n = \frac{\lambda x}{\lambda y}$	Ratio of grid spacing
I_x	The moment of inertia in the x direction of a plate or girder – in ⁴
I_y	The moment of inertia in the y direction of a plate or girder – in ⁴
K_{tx}	Torsional Constant of a plate or girder in x direction – in ⁴
K_{ty}	Torsional Constant of a plate or girder in y direction – in ⁴
E	Modulus of elasticity of the material of the plate or girder – ksi
G	Modulus of rigidity of the material of the plate or girder – ksi
$D_x = \frac{E I_x}{\lambda}$	Measure of the bending stiffness of a plate or girder in x direction – K in ² /in.
$D_y = \frac{E I_y}{n \lambda}$	Measure of the bending stiffness of a plate or girder in y direction – K in ² /in.
$H_x = G \frac{K_{tx}}{\lambda}$	Measure of the torsional stiffness of a plate or girder in x direction – K in ² /in.
$H_y = G \frac{K_{ty}}{n \lambda}$	Measure of the torsional stiffness of a plate or girder in y direction – K in ² /in.
$2H = G \left(\frac{K_{tx}}{\lambda} + \frac{K_{ty}}{n \lambda} \right)$	Measure of the total torsional stiffness of a plate or girder – K in ² /in.
I_{wx}	The warping constant of a plate or girder in x direction – in ⁶
I_{wy}	The warping constant of a plate or girder in y direction – in ⁶
$C_x = \frac{E I_{wx}}{\lambda}$	Measure of warping stiffness of a plate or girder in x direction – K in ⁴ /in.

$C_y = \frac{E I_{wy}}{n \lambda}$	Measure of warping stiffness of a plate or girder in y direction – K in ⁴ /in.
$A = \frac{C_x}{\lambda^2 D_y}$	Dimensionless ratio
$B = \frac{C_y}{\lambda^2 D_y}$	Dimensionless ratio
$\alpha = \sqrt{D_x D_y}$	Dimensionless ratio
$\beta = \frac{H}{D_y}$	Dimensionless ratio
$\epsilon_x = \frac{C_y}{\lambda^2 H_y}$	Dimensionless ratio
$\epsilon_y = \frac{C_x}{\lambda^2 H_x}$	Dimensionless ratio
$\eta_x = \frac{C_y}{\lambda^2 D_x}$	Dimensionless ratio
$\eta_y = \frac{C_x}{\lambda^2 D_x}$	Dimensionless ratio
$\xi_x = \frac{H}{D_y}$	Dimensionless ratio
$\xi_y = \frac{H}{D_x}$	Dimensionless ratio
$\Phi_{xy} = \frac{H_x}{D_y}$	Dimensionless ratio
$\Phi_{yx} = \frac{H_y}{D_x}$	Dimensionless ratio
$M_{x,y}$	Bending Moment in the x or y direction – K in/in.
$M_{x,y}^T$	Total twisting moment, in the x or y direction – K in/in.
$M_{x,y}^{ST}$	St. Venant's twisting moment in the x or y direction – K in/in.
$M_{x,y}^w$	Warping twisting moment in the x or y direction – K in/in.
$V_{x,y}$	Shearing force per unit width in the x or y direction – K /in.
$R_{x,y}$	Reaction in the x or y direction – K /in.
$S_{x,y}$	The section modulus of the cross section in the x or y direction – in ³
$S_{ws(x,y)}$	The warping statical moment at a point s on a cross section in the x or y direction – in ⁴
$W_{ns(x,y)}$	The normalized warping function at a point s on the cross section in the x or y direction – in ²
$\Phi_{x,y}$	Unit twist in the x or y direction – radians
$\Phi_{x,y}''$	The second derivative of unit twist in the x or y direction – in ⁻²

$\sigma_{bx,y}$	The bending stress in the x or y direction, due to plane bending – ksi
$\sigma_{wx,y}$	The warping normal stress in the x or y direction – ksi
$\tau_{bx,y}$	The bending shearing stress in the x or y direction, due to plane bending – ksi
$\tau_{Stx,y}$	Pure torsional shearing stress in the x or y direction – ksi
$\tau_{wx,y}$	The warping shearing stress, in the x or y direction – ksi

References

1. Orthotropic Steel Plate Deck Bridges, AISC, New York, N.Y., 1963.
2. Orthotropic Bridges Theory and Design, Lincoln Arc Welding Federation, Cleveland, Ohio, 1967.
3. HEINS, C. P., LOONEY, C. T. G., Bridge Analysis Using Orthotropic Plate Theory, ASCE, Vol. 94, No. ST 2, Feb. 1968.
4. POWELL, G. H., OGDEN, D. W., Analysis of Orthotropic Steel Plate Bridge Decks, ASCE, Vol. 95, No. St 5, May 1969.
5. NARUOKA, M., On the Analysis of a Skew Girder Bridge by the Theory of Orthotropic Parallelogram Plates, I.A.B.S.E., Vol. 19, p. 231, 1959.
6. JAEGER, L., The Analysis of Grid Frameworks of Negligible Torsional Stiffness by Means of Basic Functions, Inst. of Civil Engineering, Vol. 6, p. 735, 1957.
7. YASUMI, M., NAMITA, Y., Analysis of Grid Girders by Means of Difference Equations, Osaka Univ. Tech. Repts., No. 295, Vol. 8, p. 95, 1958.
8. Yoo, C. H., Grid System Analysis by Finite Difference Technique, M.S. Thesis, Univ. of Maryland, College Park, Md., U.S.A., Aug. 1969.

Summary

The relationship between deformations and internal grid forces; bending, torsion (St. Venant and warping), shear, and applied external forces is obtained by an equivalent orthotropic plate technique. The resulting differential equations are then solved by finite differences and various computer programs, as applied to a bridge structure.

The results of a hypothetical bridge analysis are presented.

Résumé

La relation entre les déformations et les forces internes du treillis, la flexion, la torsion (St.-Venant), le cisaillement et les forces appliquées extérieures est obtenue au moyen d'une technique équivalente de plaques orthotropes. Les équations différentielles résultantes sont ensuite résolues pour des différences finies au moyen de différents programmes d'ordinateur et appliquées à des constructions de ponts.

On présente les résultats de l'analyse d'un pont hypothétique.

Zusammenfassung

Die Beziehung zwischen Verformung und inneren Kräften, Biegung, Drillung (St.-Venant- und Wölbkraft-), Schub und aufgebrachten äußeren Kräften wurde durch eine äquivalente Methode für orthotrope Platten erhalten. Die erhaltene Differentialgleichung ist sodann mittels endlicher Differenzen und verschiedenen Computerprogrammen gelöst sowie für Brücken angewendet worden.

Die Ergebnisse einer hypothetischen Brückenberechnung liegen vor.